Proceedings of the 28th IEEE
EMBS Annual International Conference
New York City, USA, Aug 30-Sept 3, 2006

Wearable Wireless Telemetry System for Implantable Bio-MEMS Sensors

Rainee N. Simons,[1] Félix A. Miranda,[2] Jeffrey D. Wilson[3] and Renita E. Simons[4]

***Abstract*—In this paper, a telemetry and contact-less powering system consisting of an implantable bio-MEMS sensor with a miniature printed square spiral chip antenna and an external wearable garment with printed loop antenna is investigated. The implantable chip antenna and the wearable garment pick-up antenna are in close proximity to each other and hence couple inductively through their near-fields and behave as the primary and the secondary circuits of a transformer, respectively. The numerical and experimental results are graphically presented, and include the design parameter values as a function of the geometry and the relative magnetic near-field intensity as a function of the angle, for the implantable chip antenna .**

I. INTRODUCTION

In human space exploration programs there are several situations such as space and planetary surface extravehicular activity (EVA), launch and de-orbit, and physical exercise in microgravity that require noninvasive monitoring of the physiological parameters, including blood pressure, heart rate, oxygen, etc. [1]. The sensors used in monitoring these parameters have to be small, light weight, wearable and inductively powered. In addition, the data from these sensors have to be wirelessly transmitted and recorded. Furthermore, the recorded data has to be periodically uploaded to a database server via a wireless local area network (LAN) for assessment. As an example, the progress to date by our group and others in the development of implantable bio-MEMS based sensor system for monitoring pressure is presented in [2]. These sensors operate in the unlicensed frequency band and the frequency, power, and range of operation as well as, the dielectric properties of the human body are summarized in Table 1. Moreover, wearable sensors and systems for unobtrusive and continuous monitoring of the vital signs of humans have recently made significant advances [3]. Hence integrating the two technologies would enable higher mobility and greater connectivity.

In this paper, a wearable wireless telemetry and contact-less powering scheme for an implantable bio-MEMS based sensor system is presented. The scheme is illustrated via a spinal implant and a wearable unit as depicted in Fig. 1. Integrated with the implantable bio-MEMS sensor and the wearable garment are a miniature (1×1 mm) printed square spiral chip antenna and a pick-up loop antenna/signal processing circuits (5×5 cm), respectively. The miniature implantable sensor antenna is modeled as a square spiral chip inductor and the computed inductance, parasitic resistance and capacitance are presented. In addition, the implantable antenna and the proximity garment pick-up antenna are coupled via the near-fields and hence the computed mutual inductance is presented. Lastly, a lumped element equivalent circuit model taking into consideration the mutual inductance, and the near-zone magnetic field intensity pattern of the implantable antenna, are presented.

TABLE 1
MEDICAL IMPLANT COMMUNICATION SERVICE BAND FOR BODY IMPLANTS AND HUMAN TISSUE DIELECTRIC PROPERTIES

Frequency (MHz)	402–405
RF Power Level External to the Body (μW) (max)	25
Range (m)	2
Human Muscle Dielectric Constant and Conductivity (S/m) at 400 MHz	58.0, 0.82
Human Fat Dielectric Constant and Conductivity (S/m) at 400 MHz	11.6, 0.08

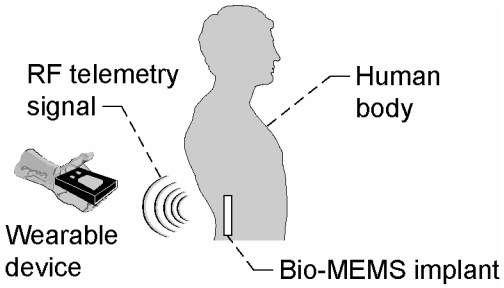

Figure 1.—Contact-less powering and telemetry concept for Bio-MEMS sensors.

II. IMPLANTABLE SQUARE SPIRAL CHIP INDUCTOR/ANTENNA

The miniature printed square spiral chip inductor/antenna is illustrated in Fig. 2 (a). A photomicrograph of the circuit fabricated on a high resistivity silicon wafer (ε_r = 11.7) is shown in Fig. 2 (b). The circuit is modeled as a series inductor L_S and resistor R_S in parallel with a capacitor C_S. The L_S is

[1]R. N. Simons, NASA Glenn Research Center, 21000 Brookpark Road, Cleveland, Ohio 44135, USA (216–433–3462; fax: 216–433–3478; e-mail: Rainee.N.Simons@nasa.gov).

[2]F. A. Miranda, NASA Glenn Research Center, 21000 Brookpark Road, Cleveland, Ohio 44135, USA (216–433–6589; fax: 216–433–3478; e-mail: Felix.A.Miranda@nasa.gov).

[3]J. D. Wilson, NASA Glenn Research Center, 21000 Brookpark Road, Cleveland, Ohio 44135, USA (216–433–3513; fax: 216–433–3478; e-mail: Jeffrey.D.Wilson@nasa.gov).

[4]R. E. Simons, John Carroll University, 20700 North Park Boulevard, University Heights, Ohio 44118, USA (440–547–0365; fax: 216–433–3478; e-mail: rsimons06@jcu.edu).

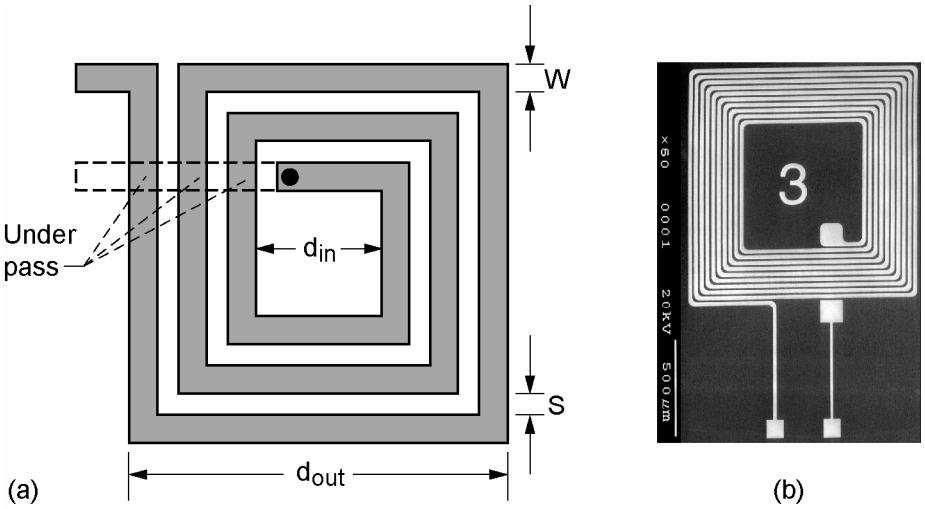

Figure 2.—(a) Schematic of a miniature spiral inductor/antenna. d_{in} = 0.5 mm, S = 10 μm, conductor is gold and thickness = 1.5 μm. (b) Photomicrograph of inductor/antenna.

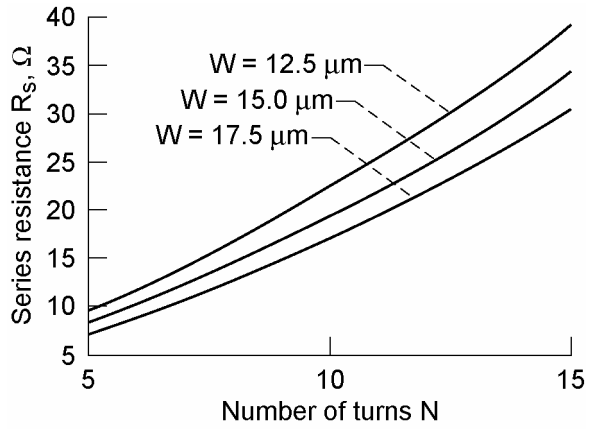

Figure 3.—Series resistance as a function of the number of turns.

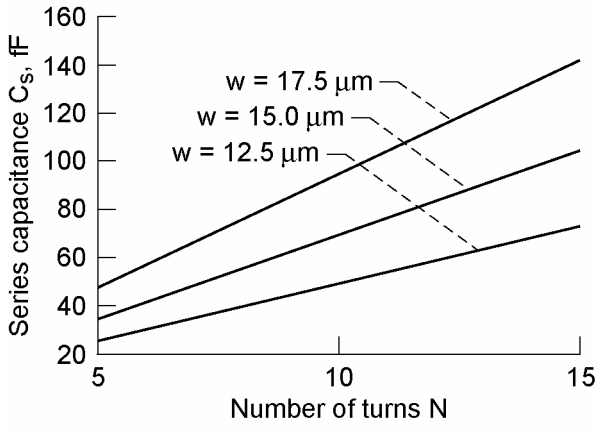

Figure 5.—Series capacitance as a function of the number of turns, the insulating dielectric is polyimide (ε_r = 3.5) and thickness = 1 μm.

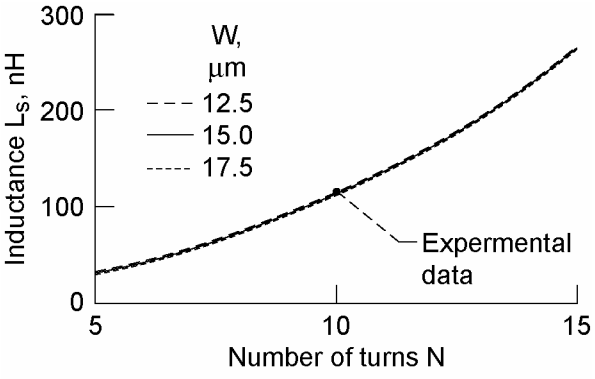

Figure 4.—Inductance as a function of the number of turns.

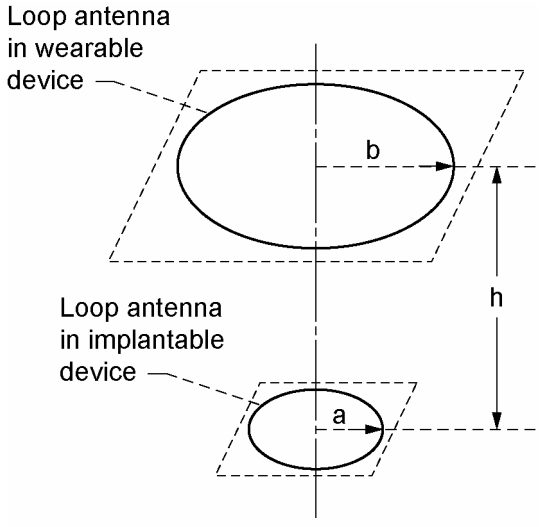

Figure 6.—Inductively coupled coaxial circular loop antennas in air.

computed using the current sheet expression given in [4] and the R_S and C_S are computed using the expressions given in [5]. In computing R_S the conductor thickness is assumed to be equal to one skin depth at the operational frequency of 403 MHz. The computed R_S, L_S, and C_S as a function of the strip width W and the number of turns N for a fixed strip separation S are presented in Figs. 3 to 5, respectively. The experimental data point in Fig. 4 is for the inductor shown in Fig. 2(b).

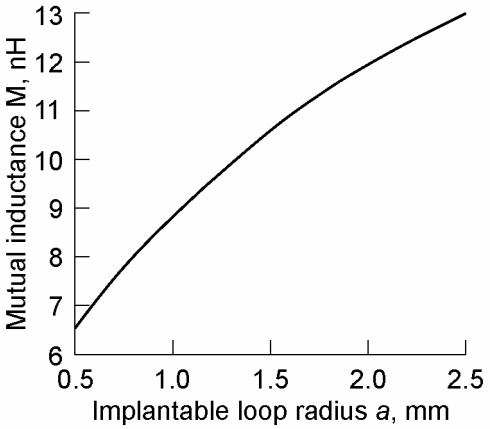

Figure 7.—Mutual inductance as a function of the implantable loop radius for h = 5 cm and b = 2.55 cm.

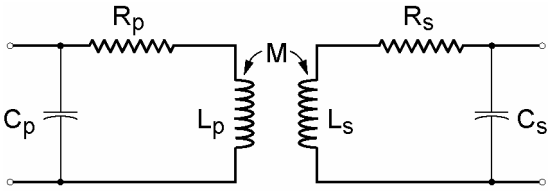

Figure 8.—The inductivity coupled loop and spiral are modeled as an equivalent transformer circuit, R_p = 3.45 Ω, L_p = 0.43 μH.

III. Equivalent Circuit Model for Inductively Coupled Square Spiral Chip and Loop Antennas

To determine the mutual inductance M, the miniature printed square spiral chip inductor/antenna and the pick-up loop antenna are modeled as two circular filamentary current paths of radius *a* and *b*, respectively, as shown in Fig. 6. Based on the expression in [6], the computed M as a function of the implantable antenna radius *a*, for a fixed separation h, is presented in Fig. 7. In addition, the inductively coupled spiral and loop antennas are modeled as an equivalent transformer [7] as shown in Fig. 8. In this model, R_p and L_p represent the loss resistance and self-inductance of the external pick-up loop antenna. The capacitance C_p is part of the input impedance matching circuit. This model would be used to compute the input impedance for designing a matching circuit.

IV. Near-Field Pattern of Implantable Square Spiral Chip Antenna Array

The case of a single miniature square spiral chip antenna has been analyzed and presented in [7]. To provide greater circumferential coverage along the torso our implantable sensor has two miniature square spiral chip antennas, with equal amplitude and phase excitation, as illustrated in Fig. 9. For the purpose of analysis, the individual chip antennas are approximated by a single turn loop of radius *a*, with constant current distribution I_0, and circumference less than one-tenth of a wavelength. Under this assumption the near-zone magnetic fields are given by the expressions in [8]. From these expressions the total near-zone magnetic field as a function of the azimuth angle θ is computed and presented in Fig. 10. A practical sensor will be housed inside a biocompatible package. This package would be constructed typically from metal/ceramics and may have curved boundaries. Hence, additional simulations are necessary to accurately predict the near-zone magnetic field intensity around the package. These simulations are done using the

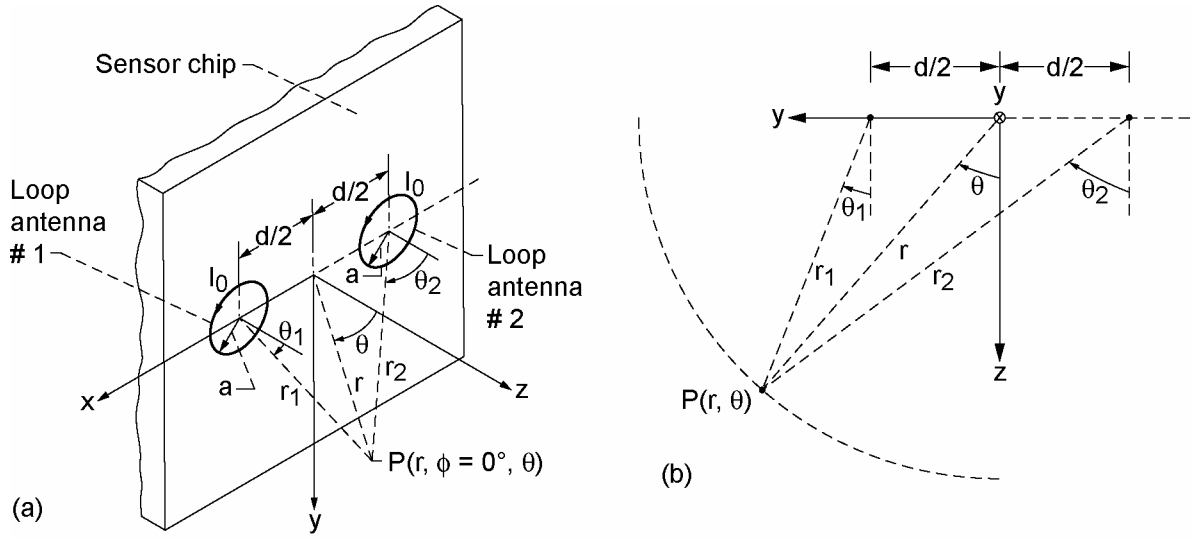

Figure 9.—(a) Sensor antenna array, a = 1mm, d = 2.5 mm. (b) Coordinate system for computing the near field.

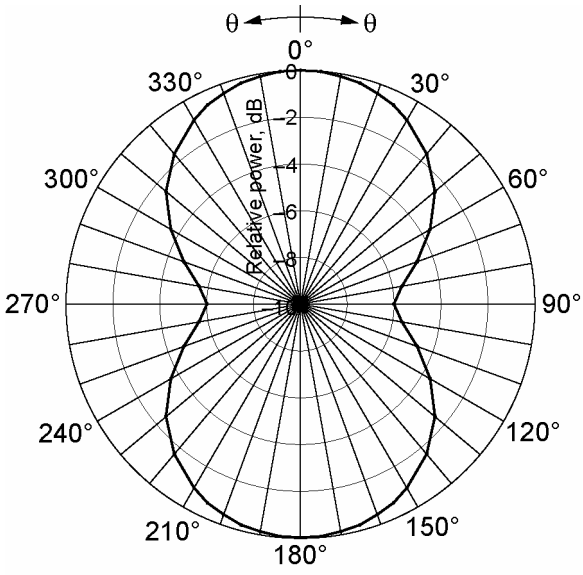

Figure 10.—Computed near-field total magnetic field component in the x-z plane, frequency = 403 MHz, r = 10 cm and I_0 = 1 mA.

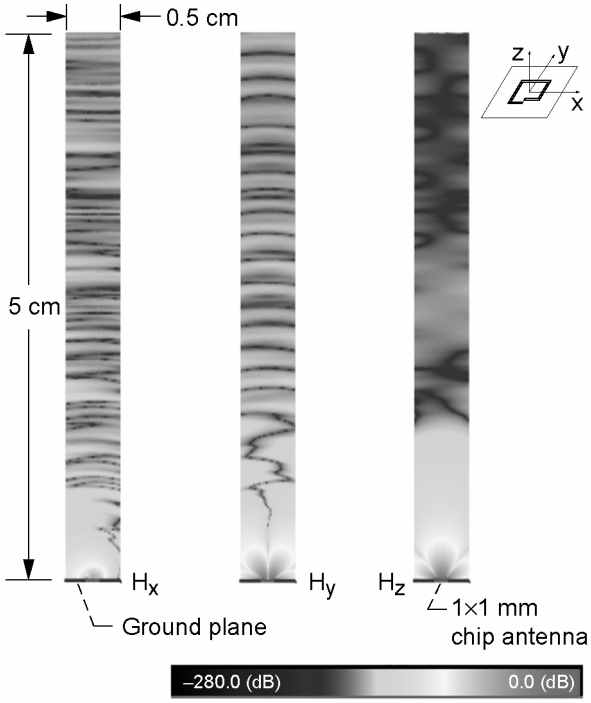

Figure 11.—Simulated intensity of the magnetic field components as a function of the distance from the center of a single-turn spiral antenna in the y-z plane. Frequency = 403.5 MHz, S = W = 15 μm, d_{out} = 1.0 mm, substrate thickness and relative permittivity are 325 μm and 11.7.

full-wave three-dimensional finite difference time domain electromagnetic analysis software, Remcom XFDTD [9]. In Fig. 11 a span shot of the simulated intensity of the magnetic field components, H_x, H_y, and H_z after one RF period, as a function of the distance from the center of a single-turn spiral antenna in the y-z plane, is presented. The maximum distance is 5 cm in the z-direction, which is typical for positioning a receiver in a wearable sensor application. The results for a multi-turn spiral will be presented in a future paper.

V. Discussions and Conclusions

A wearable wireless telemetry and contact-less powering scheme for an implantable bio-MEMS based sensor system is presented. A miniature printed square spiral chip antenna and a printed loop antenna are integrated with the sensor and the wearable garment, respectively for telemetry and inductive powering. The implantable sensor antenna is modeled as a square spiral chip inductor. The computed results presented include the inductance, the parasitic resistance and capacitance and the near-zone magnetic field intensity pattern, of the implantable antenna array. In addition, for the coupled chip and loop antennas, the mutual inductance and an equivalent circuit model are presented.

As a concluding remark it may be mentioned that the miniature transmitters and receivers required for implantable sensor telemetry can be realized in sub-micron RF CMOS technology with DC power consumption on the order of few hundred microwatts [10], [11].

References

[1] C. W. Mundt, et al., "A Multiparameter Wearable Physiologic Monitoring System for Space and Terrestrial Applications," IEEE Trans. Info. Technology in Biomedicine, Vol. 9, No. 3, pp. 382–391, Sept. 2005.

[2] R. N. Simons, D. G. Hall, and F. A. Miranda, "RF Telemetry System for an Implantable Bio-MEMS Sensor," IEEE MTT-S Inter. Microwave Symp. Dig., Vol. 3, pp. 1433–1436, Fort Worth, TX, June 6–11, 2004.

[3] P. Bonato, "Wearable Sensors/Systems and Their Impact on Biomedical Engineering," IEEE Engineering in Medicine and Biology Magazine, Vol. 22, No. 3, pp. 18–20, May/June 2003.

[4] S. S. Mohan, M. D. M. Hershenson, S. P. Boyd, and T. H. Lee, "Simple Accurate Expressions for Planar Spiral Inductances," IEEE Jour. Solid-State Circuits, Vol. 34, No. 10, pp. 1419–1424, Oct. 1999.

[5] M. D. M. Hershenson, S. S. Mohan, S. P. Boyd, and T. H. Lee, "Optimization of Inductor Circuits via Geometric Programming," Proc. 36th Design Automation Conf., pp. 994–998, New Orleans, LA, June 21–25, 1999.

[6] S. Ramo, J. R. Whinnery and T. V. Duzer, Fields and Waves in Communication Electronics, 3rd Edition, New York, NY: John Wiley and Sons, 1994, Section 4.7 and Example 4.7a.

[7] R. N. Simons and F. A. Miranda, "Modeling of the Near-Field Coupling Between an External Loop and an Implantable Spiral Chip Antenna in Biosensor Systems," Accepted for presentation at the joint 2006 IEEE AP-S Inter. Symp. Antennas & Propagation and USNC/URSI National Radio Science and AMEREM Meetings, Albuquerque, NM, July 9–14, 2006.

[8] C. A. Balanis, Antenna Theory Analysis and Design, 2nd Edition, New York, NY: John Wiley and Sons, 1997, section 5.2.4, equations (5-24), Example 5.2, and equation (5-37a).

[9] http://www.remcom.com.

[10] R. Rofougaran, T. H. Lin, F. Newberg, and W. J. Kaiser, "A Micro-Power CMOS RF Front-End for Embedded Wireless Devices," 1999 IEEE Radio Frequency Integrated Circuits Symp. Dig., pp. 17–20, Anaheim, CA, June 13–15, 1999.

[11] N. M. Neihart and R. R. Harrison, "Micropower Circuits for Bidirectional Wireless Telemetry in Neural Recording Applications," IEEE Trans. Biomedical Engineering, Vol. 52, No. 11, pp. 1950–1959, Nov. 2005.